Modelling hot cracking in 6061 aluminium alloy weld metal with microstructure based criterium

Aurélie Niel, Cyril Bordreuil, Fréderic Deschaux-Beaume, Gilles Fras

Modeling hot cracking phenomena in 6061 Aluminum alloy weld with a microstructural based criteria

A.Niel, C.Bordreuil, F.Deschaux-Beaume, G.Fras
Laboratoire de Mécanique et Génie Civil, Université Montpellier 2, Montpellier, France
cyril.bordreuil@univ-montp2.fr

Abstract
Hot cracking in welding is a complex phenomena due to coupling between process, metallurgy and mechanical loading. In this paper, a coupled approach that integrates microstructural prediction based on the process simulation and criteria at the microstructural scale is proposed. The criteria is based on some development of Rappaz et al [1] and takes into account the influences of grain morphology, mechanical and thermal fields induced by welding, on hot cracking. To integrate all factors influencing hot cracking, a methodology is developed that couples process simulation, simple microstructural prediction and criteria along columnar grains. The criteria based on the microstructure behavior is able to predict crack onset location in columnar grains zones.

Introduction

To increase productivity in welding, the welding speed could be increased. Unfortunately, even with increasing power, defects as hot cracking can appear. Numerous works investigated hot crack phenomena and even workshops are dedicated to it [2]. The mechanism is not yet well predicted due to the complex phenomenon influencing it.
Hot cracking appears in the Brittle Temperature Range (BTR) defined as the temperature interval where the microstructure is in a critical configuration. The material is solidifying and liquid and solid phase are mixed. The material in the BTR is in a high solid fraction state and can sustain mechanical loading. At this solid fraction, the liquid can hardly flow around the solidifying solid skeleton and the liquid accommodate with difficulties tensile deformation or solidification shrinkage induced by the process. This phenomena in welding is difficult to predict due heterogeneous fields and microstructure due to localized heat input induced by the welding process. For example, the microstructure generation and behavior under solidification is directly related to the heat transfer. For the mechanical point of view, strain state is complex around the weld pool [3]. To understand hot cracking, these phenomenon have to be included in the analysis.
To characterize hot crack during welding, many tests were done. Two tests are mainly used. The JWRI tests [4] plays on geometrical singularity to create or stop a hot crack. The varestrain [5] plays on a non homogeneous loading on the solidification zone. Because the tests leads to complex and even singular strain state, numerical simulation must be used.
To better understand the coupling between metallurgy, thermal and mechanical fields, simulation and modeling effort is necessary. An integrated approach is then developed that coupled solidification, thermal and mechanical fields analysis to differentiate the influence of each phenomena, in a numerical model. In this paper, a method that coupled process simulation with a simple microstructural model based on the arrest of columnar grain growth is presented. The columnar grain are predicted based on geometrical consideration. Once the microstructure is predicted a criteria similar to the one developed by [1] is applied along the columnar grains to detect the critical location. This adaption of RDG criteria to welding that couples metallurgical prediction and welding process simulation is a new methodology.
The paper is organized as followed. First, the hot cracking test [6] is reminded together with some metallurgical consideration. The modeling is then presented, starting with the process simulation. Then,

the microstructural prediction is detailed. To know the critical location for hot cracking, the Rappaz et al [1] is adapted to the case of welding with large heterogeneity of fields and is written in the columnar grain frame. Finally, the criteria is used with microstructural prediction and thermal and mechanical fields coming from the process simulation to appreciate the capacity of the model to describe hot cracking tests.

Experimental setup and welding conditions

Niel et al [6] has developed a new hot cracking test similar to the PVR test [7]. The test consists to perform a tensile loading before welding in the direction of welding (fig 1). The specimen to be tested is a thin 6061 Al Alloy plate. The welding parameters for autogeneous weld bead are chosen to have full penetration. Many tests were performed with and without tensile loading with different process parameters. The cracks are always initiated in quasi-steady state thermal zone (fig 2) in the columnar grains. In this work, two different tests are reported and will be used to appreciate the ability of the criteria to describe the crack onset. The parameters are shown in table 1. The test A has no cracks whereas test B has cracks. The only parameter modified between the two tests is the current. The current plays an important role in the thermal transfer and on the weld microstructure. The plate are 3mm thick and the geometry is 400x50mm. The autogeneous weld bead is done in a symmetric way for 300mm length. The imposed displacement is around 1mm and creates a tensile stress in the specimen. The welding speed is high and is necessary to promote hot cracks.

For the two tests, the microstructure in the weld pool is almost the same (fig 3). Equiaxed grain are in the middle of the weld bead whereas columnar grains are on the side. Due to fast cooling rate, the grains are dendritic with small second arm [6, 8]. To compare weld pool from a metallurgical point of view, the weld pool width, the equiaxed grain zone width, the width of the columnar grain, and the mean orientation of columnar grain are reported in table 2. The size of the weld pool increased with the intensity and the different width are also modified. The final microstructure is related to weld pool solidification. The microstructural morphology is obtained different mechanisms taking place at the weld pool border and governed by thermal loading. First, the columnar grains started to grow from the base material by epitaxy and sites are nucleated in the center of the weld pool due to a high undercooling [9]. There is a competition between growth of columnar grain and nucleation and growth of equiaxed grains. Experimentally, it is difficult to observe microstructure generation under welding. Some high speed imaging were done and will be used to appreciate crack onset in the results section.

Post-mortem analysis showed that the cracks are located at inter grain boundaries and no liquid seems to be present. It seems that the crack onset for 6061 Al Alloy is due to lack of liquid feeding.

Modeling

Thermal process simulation

Because the weld are fully penetrated, a two dimensional mesh model was realized. The heat input was represented by a Gaussian distribution with a circular section with a radius of 3mm and an efficiency of 60%. These parameters was calibrated with thermocouples measurement and post mortem micrography. The mean thermal coefficients used are given in table 3. The thermal field are given by a thermal conductive model and the weld pool convection is not taken into account. More details can be found in [10]. The thermal and plastic strain rate field histories are stored in order to be used for microstructural prediction and in the hot cracking criteria (section results).

Mechanical process simulation

The 6061 behavior was identified by Maisonnette [11] in a wide range of temperature. The plasticity seems to exhibit a mixed kinematic and isotropic behavior in this range. The curves and the mechanical behavior identified in [11] are entered in finite element code. The main coefficients used in the mechanical simulation are shown in table 4. The localized heat input loads the plate and generates plasticity in the vicinity of the weld pool. Some plastic strain (rate) are showed in fig.4. The strains are shown at different locations in and near the weld pool. Depending on the location, different strain rate components are studied. At the weld pool border, the strain component in the direction of welding (direction 2) are looked at and the strain component perpendicular (direction 1) in the center of the weld pool is analyzed. In the border of the weld pool, columnar grains are dominant and are almost perpendicular to the weld direction. Plastic strain rate 22 leads to an opening of the interdendritic spacing into or between columnar grains. At high temperatures, the material is in a solid and liquid state exhibiting a dilatation plasticity not taken into account in the model. This behavior decreases normally the plastic strain rate. As explained by Chihosky [2], some structural effects load the material in the last stage of solidification. High 22 plastic strain rate in columnar grain can be attributed to incompatible deformation between this zone and its neighborhood. In particular, the zone in border of the weld pool is mainly strained at the front of the weld pool leading to plastic stain that are not restaured after the weld pool has passed. When the columnar dendrites starts to be loaded, the plastic strain must accommodate plastic strain in the weld pool border.

Microstructure prediction

For the prediction of grain structures during solidification, the most successful techniques developed so far have employed the cellular automata approach [1]. In the present paper, a simpler approach based on geometry and an analytical model developed by Hunt for the columnar to equiaxed transition is chosen to determine the width of the different zone. The columnar to equiaxed transition is a complex solidification phenomenon that is related to cooling rate and competition between columnar growth and nucleation in the center of the weld pool. We will discuss more microstructure phenomena in modeling section. This approach with poor physical ingredient allows nevertheless fast computation.

A dedicated numerical procedure is developed. First, a layer is defined to keep all microstructural evolutions. The layer is defined as quadrangle domain superimposed to the process domain and is located in the quasi steady state part of the thermal field. In this layer, the thermal fields (Temperature and gradient) are interpolated on a grid to find the liquid isotherm. In this work, it is assumed that this isotherm is the weld pool border and the set of point is noted P_{weld} . The weld bead is determined with the envelope of the weld pool . The envelope is determined by the set of points P_{border} that are in the border of the weld pool. Weld pool solidification parameters are the thermal gradient G, the growth rate R and the undercooling ΔT [8]. The physical phenomenon influenced by these parameters are the nucleation, the growth and eventually the coalescence of grains. Due to rapid solidification, the microstructure is dendritic and the laws of kinetic are extrapolated from those obtained at equilibrium. The microstructure generation is a competition between the nucleation phenomena and the growth of grains. Based on Hunt work, Kurz proposed [13] an analytical model to predict the CET for fast cooling rate. According to this criterion the microstructure will be predominantly columnar when:

$$g = G^n / V > Cst \qquad (1)$$

where n and Cst are constant depending on the alloy system. With other simulation, this two parameters are estimated at 1./10 and 0.2 respectively. The criteria (eq (1)) is computed on the liquid isotherm that is computed on the microstructural layer on points P_{weld} . The value of the gradient at time t is also interpolated on these points . The solidification speed (V) is computed with the direction of welding and the local normal to the weld pool border at points P_{weld} [14]. Based on the criteria Eq (1) is computed on this contour. The point of transition P_{CET} between equiaxed and columnar grain is

found for time t. Then, the point is pushed back in a list that contains the segments belonging to the border between columnar and equiaxed zone. The sets of points that determined the morphology of the weld bead is shown in fig 4. The equiaxed zone is defined between the center of the weld pool and the points P_{CET} and the columnar zone is defined between these points P_{CET} and the set of points P_{border} .

Columnar grains are modeled as segments which represents the skeleton of the grains and equiaxed grains are modeled as polygons. In the equiaxed zone, the grains are generated by putting sites inside the domain and then by performing a constrained voronoi of the domain in order to have polygons. To put site in the domain, a mesh procedure is used. This procedure is able to modify locally the size of the mesh in function of an external field. Experimental analysis [6] have shown that the grain size is constant in the equiaxed zone. So the size of the mesh is set constant and equal to the grain size that was measured. This procedure is not predictive but the equiaxed zone is not used anymore in the criteria developed further. The critical point for the criteria is the columnar zone. Because base material is not taken into account in this simple metallurgical model, a characteristic length corresponding to the width of columnar grain starting from the base material must be set in order to create the columnar grain. Once the columnar grain are initiated at the weld pool border on the set P_{border} with this length, the growth of the columnar grain must be modeled. During one time step, the segment is advanced until it reached the weld pool border. The direction of advance is taken by a simple law where the angle tends to align with the heat flux:

$$\dot{\alpha} = a\left(\alpha - \alpha_{heat\ flux}\right)$$

where α is the angle of the direction of first arm of dendrites in the global frame. The coefficient a is determined with the first test A and is identified around 0.25. The thickness of each grain is determined with the solid fraction that is based on Scheil Gulliver law. This simple model is questionable regarding physical background but one purpose of the work is to adapt a criteria developed by Rappaz, Drezet and Gremaud [1] on columnar grains during welding. This algorithm for geometrical prediction of the microstructure is reminded in table 5. Once initiated, each columnar grain are stored in a list and each grain has an index to know if it is stopped or still in growth. Each columnar grain skeleton is composed of several segments and each segment has an index to know if the segment is partially melt or solid.

Criteria for hot cracking in columnar grains

Rappaz, Drezet and Gremaud [1] developed a hot tearing criterion based upon mass balance over the liquid and solid phases. This criterion takes into account tensile deformation and the solidification shrinkage. The criterion can reproduce A curve for variable concentrations. This criterion was written in isotherm frame. In this paper, the criterion is rewritten in frame of columnar grains and a weak formulation is proposed that allow to take into account the variation of plastic strain and thermal fields along a columnar grain. Rappaz, Drezet and Gremaud proposed to take into account mass conservation on a Small Element Volume (SEV) where the principal direction is oriented in the primary dendrite arm direction. On fig 6, the SEV is shown. The SEV is characterized by the different quantities : the velocity of the liquid in the solid skeleton v_l , v_s the velocity of the solid phase and the solid fraction f_s . v_l is mainly the component of fluid velocity in the direction of first dendrite direction.

If the mass conservation is written in the frame of the solid liquid SEV, it is:

$$\partial\langle\rho\rangle/\partial t + dive\langle\rho v\rangle = 0 \quad (2)$$

where <.> stands for the mean value over the phases. If f_l is the liquid fraction, the mean value for density can be written: $\langle\rho\rangle = \rho_s f_s + \rho_l f_l$ where ρ_s and ρ_l are the solid and liquid density. The second term in equation correspond to the mass flow. The mass flow inside the SEV is only possible through liquid and plastic straining of the solid skeleton:

$$dive\langle \rho v \rangle = \partial \rho_l v_{l\xi}/\partial \xi + \partial \rho_s v_s/\partial \eta$$

Rappaz showed that $\partial \rho_s v_{s\xi}/\partial \eta = \dot{\varepsilon}_p$ where the plastic strain rate is perpendicular to the columnar direction and the gradient of the fluid flow is given by the Darcy's law:

$$\partial \rho v_{l\xi}/\partial \xi = -K\, dp/d\xi$$

where K is the permeability. In this work the permeability is given by a Carman-Kozeny approximation [1] :

$$K = \lambda_2^2 (1-f_s)^3/180/f_s^2$$

with λ_2 the second arm spacing taken as those observed on the microstructure (50 micrometer). Combining these equations leads to:

$$-K\, dp/d\xi + \partial f_s/\partial T\, \dot{T} + (1+\beta)\dot{\epsilon}_p = 0 \quad (3)$$

where $\beta = \rho_s/\rho_l - 1$ is the solidification shrinkage coefficient. The density are given in tab.3. This equation defers to the one proposed by Rappaz et al [1] due to the lack of transport term. This equation can not be solved everywhere so a weak formulation is performed on it with the pressure as degree of freedom. The microstructure prediction gives the skeleton of the columnar grain along which the equation (3) can be integrated. In the case of welding $\dot{\varepsilon}_p$ and T fields are heterogeneous. To solve this equation, the second and third term of equation (3) are known from the simulation at each point of the columnar grain by an interpolation procedure. The skeleton is naturally divided into segments. Each segment is the support for linear interpolation and then two gauss points are used to integrate the weak formulation. The linear interpolation shape function is chosen as a test function. The equation (3) is multiplied by the test function and then integrated by parts to lead :

$$\int_L [\boldsymbol{B}]^T K [\boldsymbol{B}] dL \,[\boldsymbol{p}] = \int_L [\boldsymbol{N}]^T (\partial f_s/\partial T\, \dot{T} + (1+\beta)\dot{\epsilon}_p)\, dL \quad (4)$$

where L is the length of a segment of the skeleton of the columnar grain. This equation has to be augmented by some boundary conditions. In general, it is assumed that the part of the columnar grains interacting with the metal liquid is a low solid fraction region so that it is surrounded by fluid at atmospheric pressure. Then the tip is imposed at atmospheric pressure. The left hand side of the equation gives a elementary matrix over the segment and the right hand side an elementary vector corresponding to source terms. Then, the matrices can be assembled all along the skeleton for the segment in the partially melt state. Then this equation is solved for every columnar grain. In equation (4), the morphology is integrated through the length of the segments and the material is integrated through the dependence of the solid fraction through temperature. Then the process is taken into account through the microstructural morphology and through the temperature rate and the plastic strain rate.

The procedure to solve the equation is shown in tab 6. Once the pressure or pressure drop is known in all the columnar grains, critical grains can be determined by looking at the highest depression in all the grains.

Results

First, the microstructural predictions are shown followed by the application of the criteria to the predicted microstructure. microstructural prediction are shown in fig 7. In this figure the red columnar grains correspond to those at temperature in the interval of solidification. Others colors are for columnar grain in solid state. On fig.7, the shape of the columnar grains can also be appreciated. The two microstructures for the two tests are shown on fig 8. As observed experimentally, the weld pool is larger for test B due to higher intensity. The prediction on the second test are in good agreement with experimental observations (see tab 2 and tab.7). The equiaxed and columnar grains widths are of the same order of magnitude as those observed experimentally. Then, the skeleton of each columnar grain are extracted from the metallurgical prediction and transformed in the one dimensional multiphase

element defined in the precedent section. The pressure is determined along the skeleton in the different part of the columnar grain in the solidification range. One of the interesting point of RDG model is that it takes into account the microstructure with the solid fraction, the change of state with the solidification shrinkage coefficient β and the plastic strain rate in perpendicular direction of the columnar grain. The model can then determined depression in the liquid network. The morphology of the columnar grain is taken into account by the orientation and the length of the columnar grain. The strain rate distribution in the mushy zone is complex and the loading of the columnar grain also. On fig 9, perpendicular plastic strain rates are shown with respect to time for a critical columnar grain in test B. The plastic strain rate is heterogeneous and demonstrates the structural effects taking place during the solidification. On fig 9, the plastic strain rate is low at the end of solidification just at crack onset. If an analysis of the source terms (terms on the right hand side of equation 4), for this test and this columnar grain, the dominant term is the one due to solid fraction with the solidification shrinkage coefficient and the contribution of plastic strain rate is low.

Pressure in the columnar grain is computed through the weak formulation presented in the last section. A criteria for the max depression can be used to detect the critical site. A simple depression criteria is expressed:

$$\Delta p < \Delta p_{cav} \quad (5)$$

It means that the max depression must be greater than the cavitation pressure. The cavitation pressure is defined as 0,24MPa and is a little bit higher than those met within the literature [1]. By applying this criteria on columnar grain, the critical site can be detected. The depression is shown in fig 10. The curvilinear coordinate is from the dendrite foot to the tip. The max depression is at the foot of the columnar grain in the last stage of solidification.

In-situ observations [6] showed that cracks initiate in the last stage of the solidification of the weld pool. High speed video (fig.11) showed that crack onset at the surface are far from the weld pool. At this stage, the microstructure is coherent and can sustain mechanical strain and the solid fraction is closed to one. The fluid constitutes a continuous network in three dimension but the liquid can not flow easily due to low permeability around the solid skeleton. On fig 11, the location of the critical columnar grain given by the computation is compared with some high speed images taken during welding. The critical grain is colored in white. On simulation and on high speed images, the initiation is seen far from the weld pool. The hot crack onset is attributed to the lack of liquid feeding in region with high solid fraction.

Conclusion

In the present paper, an original model to predict hot cracking was devised. The model extended the development of Rappaz, Drezet and Gremaud [1] by applying it on microstructural prediction. The model seems to describe hot crack in 6061 Aluminium Alloy in zone in the last stage of solidification. The model takes into account the different coupling that can coexist between microstructural, process and mechanical induced mechanisms. Despite the two dimensional numerical modeling, crack onset location is well approximated.

In order to appreciate the availability of such model, the microstructural prediction was mainly based on a analytical model and on geometrical consideration. The metallurgical prediction can have improvement and can be based on cellular automata as proposed by Dress [14] and Rappaz [15].

If the model give nice prediction for the crack onset, we keep in mind that the material has three dimensional behavior.

References

[1] Rappaz.M, Drezet.JM, Gremaud.M, *A new hot tearing criterion*. Metallurgical and materials transactions A, 1999, 30A :449

[2] Hot Cracks in welding I,II,II, Bollinghaus, Lippold, Cross, Springer

[3] Chihoski.R.A, *Understanding weld cracking in aluminium sheet*. Welding Journal, January :24– 30, 1972.

[4] F. Matsuda, H. Nakagawa, and K. Sorada. D*ynamic observation of solidification and solidification cracking during welding with optical microscope (i) - solidification front and behavior of cracking*. Trans. Jap. Weld. Ins., 1982, 11 :67 – 77

[5] Savage W F, Lundin C D *Application of the varestraint technique to the study of weldability.* Welding Journal. 1965 45: 497s–503s

[6] Niel, Deschaux, Bordreuil, Fras, work in progress

[7 G. Rabensteiner, J. Tösch, H. Schabereiter: *Hot Cracking Problems in Different Fully Austenitic Weld Metals*; Welding Journal, Jan. 1983

[8] Norman.A.F, Drazhner.PM, and Prangnell.P.B , *Effect of welding parameters on the solidification microstructure of autogenous tig welds in an al alloys*. Materials Science and Engineering, 1999, A259 :53 – 64

[9] David.S, Vitek.J, *Correlation between solidification parameters and weld microstructures*, International Materials Reviews, 1989, Volume 34 , pp. 213-245(33)

[10] Niel.A, Etude et modélisation du phénomène de fissuration a chaud en soudage a l'arc : Application a l'alliage d'aluminium 6061 , Thèse de l'université Montpellier 2, 2011

[11] Maisonnette.D, *Influences mécaniques et métallurgiques de procédés hautes température s sur un alliage*. PhD thesis, INSA Lyon, 2010.

[12] Rappaz.M, Gandin.Ch-A, Probabilstic modelling of microstructure formation in solidification processes,Acta metallurgica and materiala, 1993, 41, 345-360

[13] Kurz.F, C. Bezencon, and M. Gaumann. *Columnar to equiaxed transition in solidification processing*. Science and technology of advanced materials, 2 :185–191, 2001

[14] Vitek.J, *The effect of welding conditions on stray grain formation in single crystal welds – theoretical analysis* , Acta Materialia, 2005, 5, 53–67

[15] Dress.W.B, Zacharia.T and Radhakrishnan.B, *Cellular Automata Modeling of Weld Solidification Structure*, International Conference on Modeling and Control of Joining Processes, *1993*

[16] Rappaz.M and Gandin.C.A and Desbiolles.J-L and Thévoz.Ph, Prediction of grain structures in various solidification processes, Metallurgical and materials transactions A, 1996, 27, 695-705

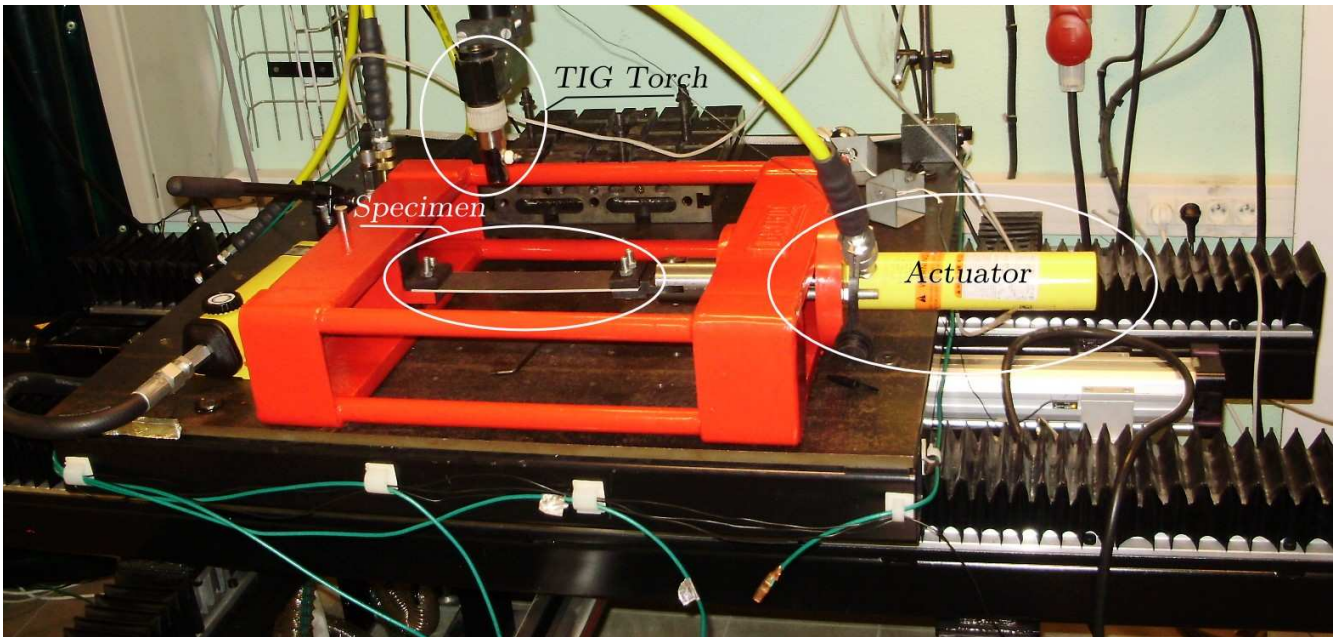

Figure 1: Hot cracking test. The welding direction and the tensile direction are given by the direction of the actuator

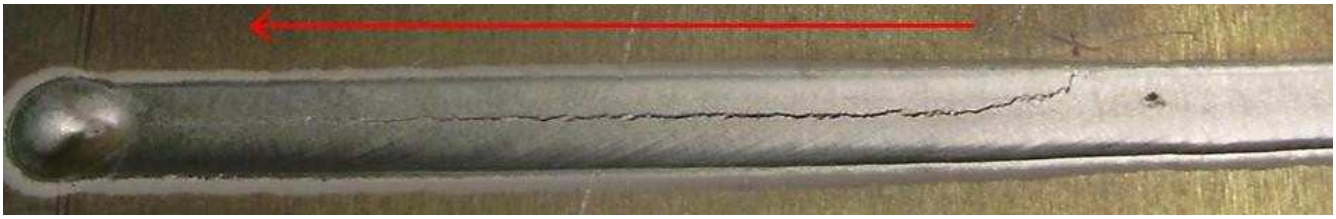

Figure 2: Autogeneous weld bead and crack location.

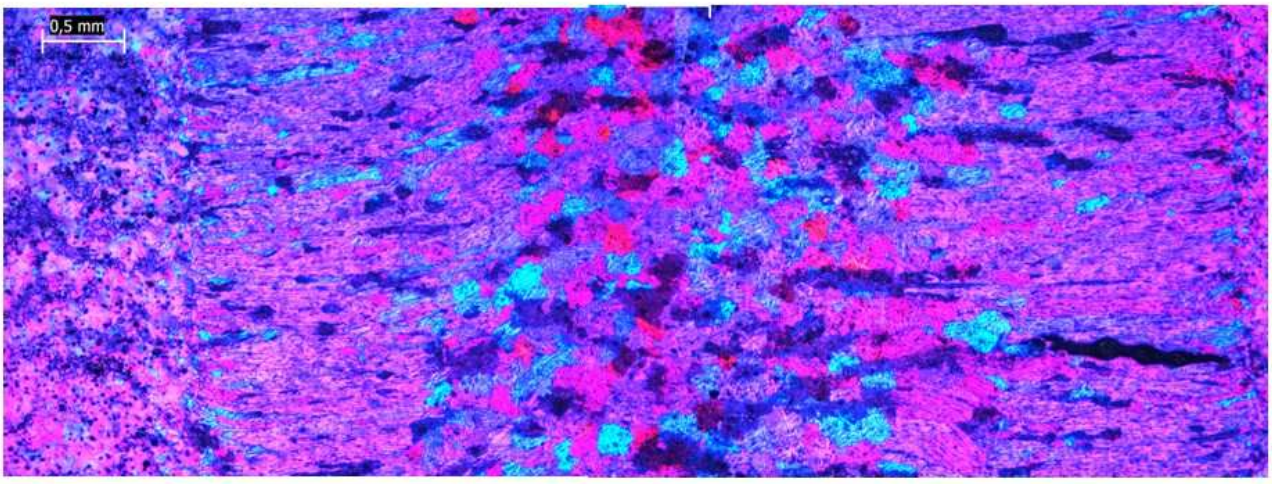

Figure 3: microstructure morphology for test A

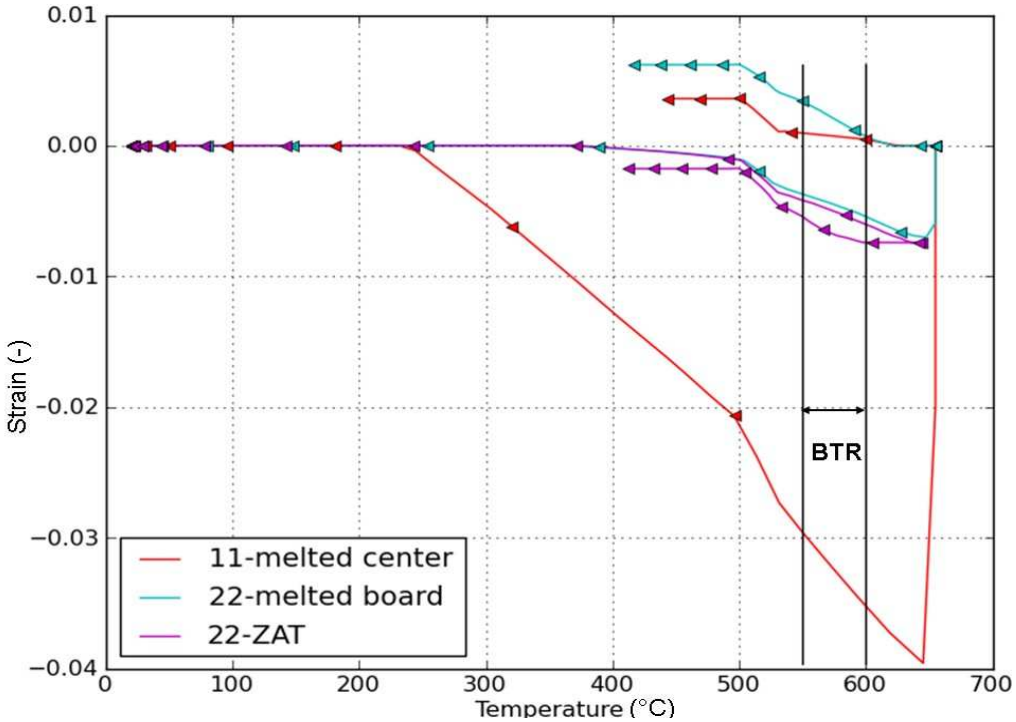

Figure 4: Plastic strain at different locations. Direction 2 is the direction of welding. At cooling the plastic strain rate is tensile for the different locations.

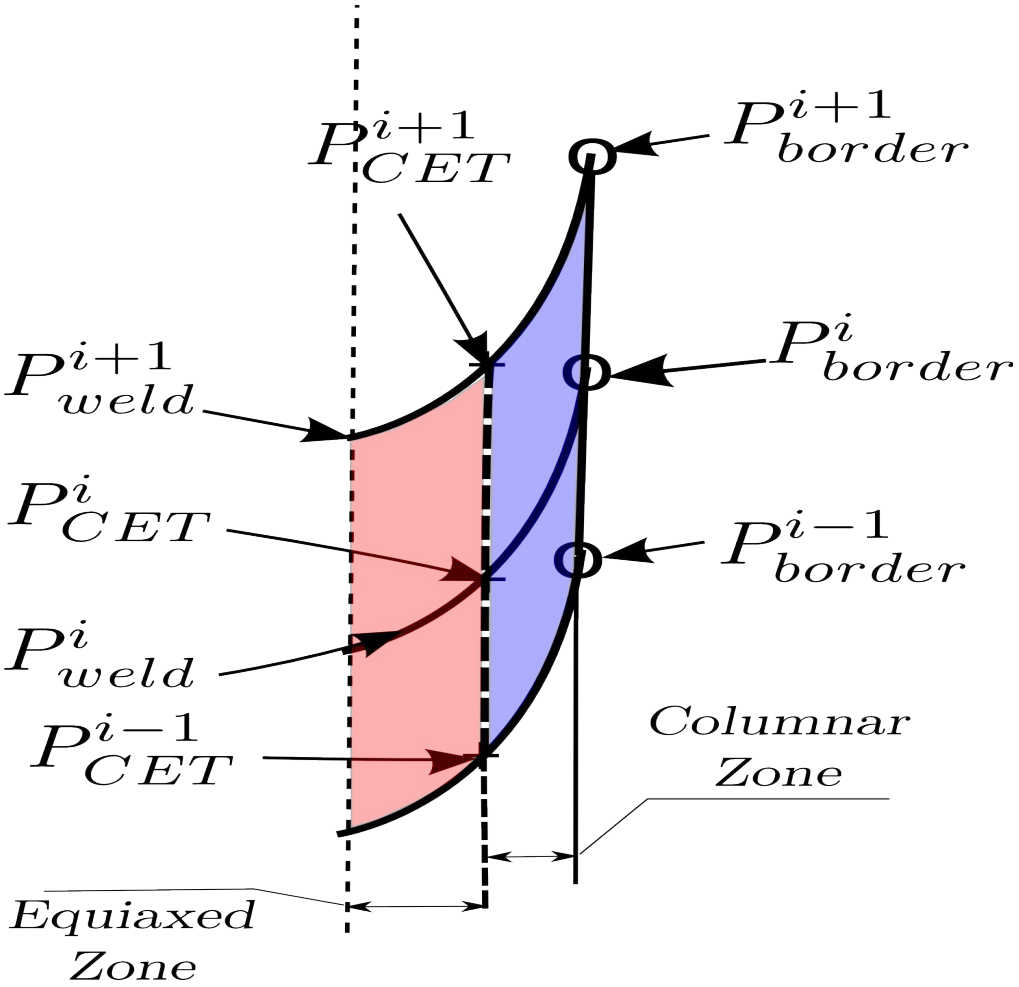

Figure 5: Geometrical points used for microstructural prediction the upper script is for time increment.

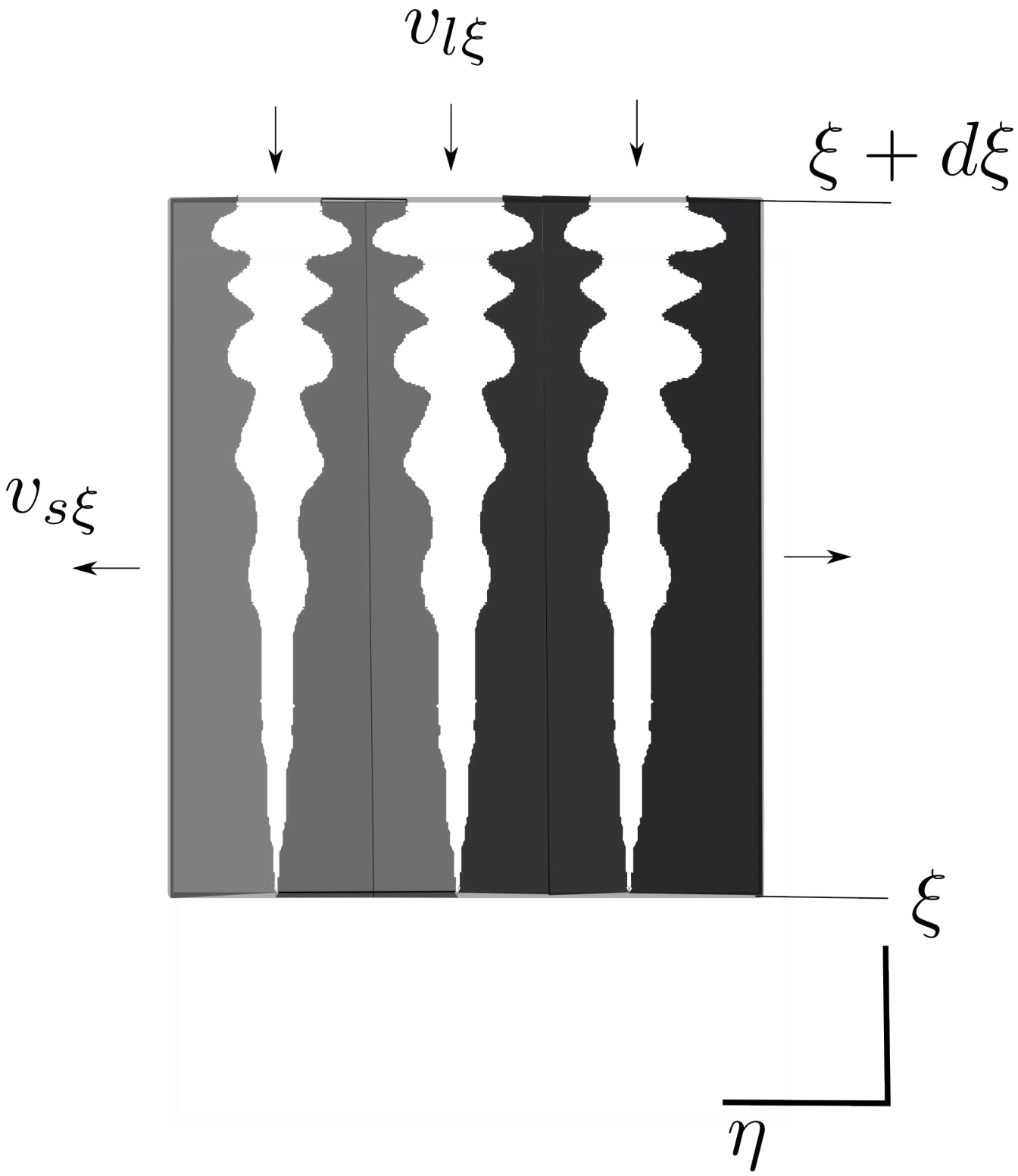

Figure 6 : Small element volume along first dendrite.

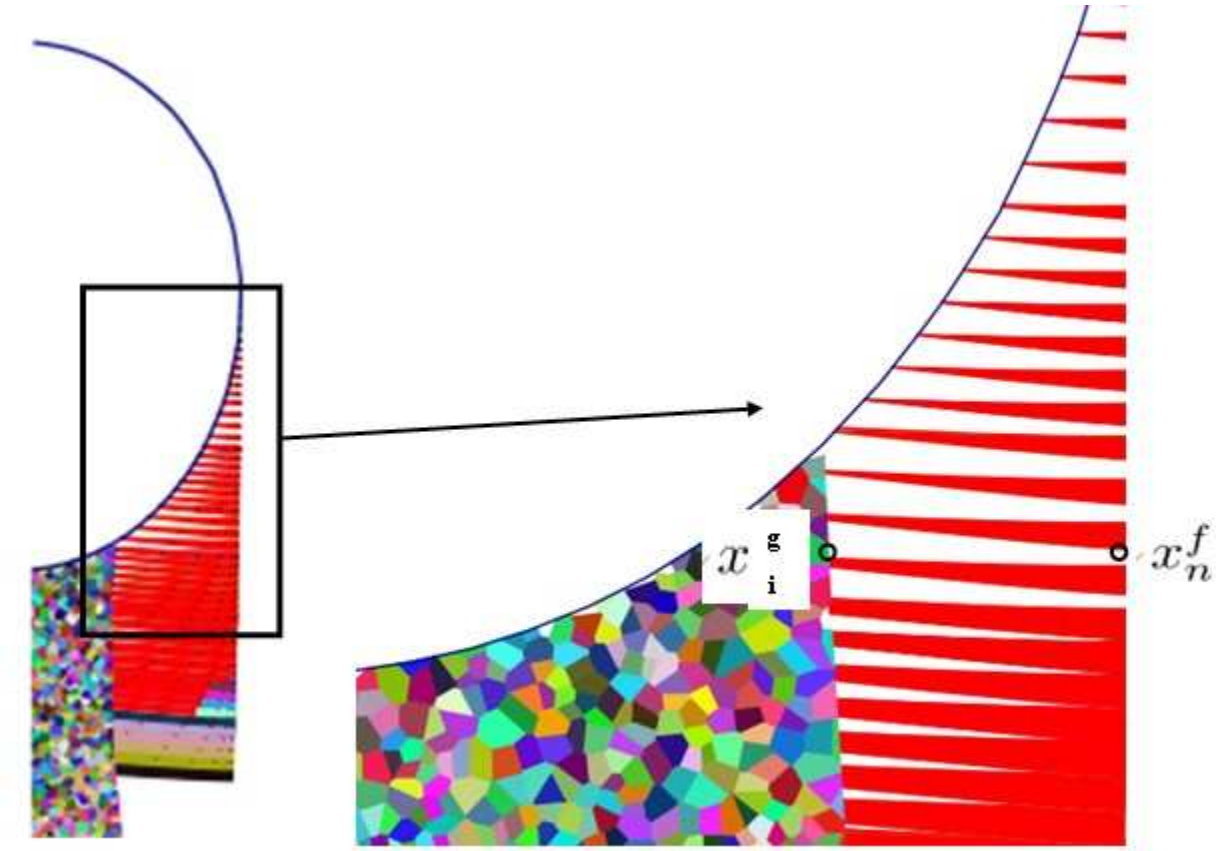

Figure 7: Columnar grains prediction based on a geometrical procedure.

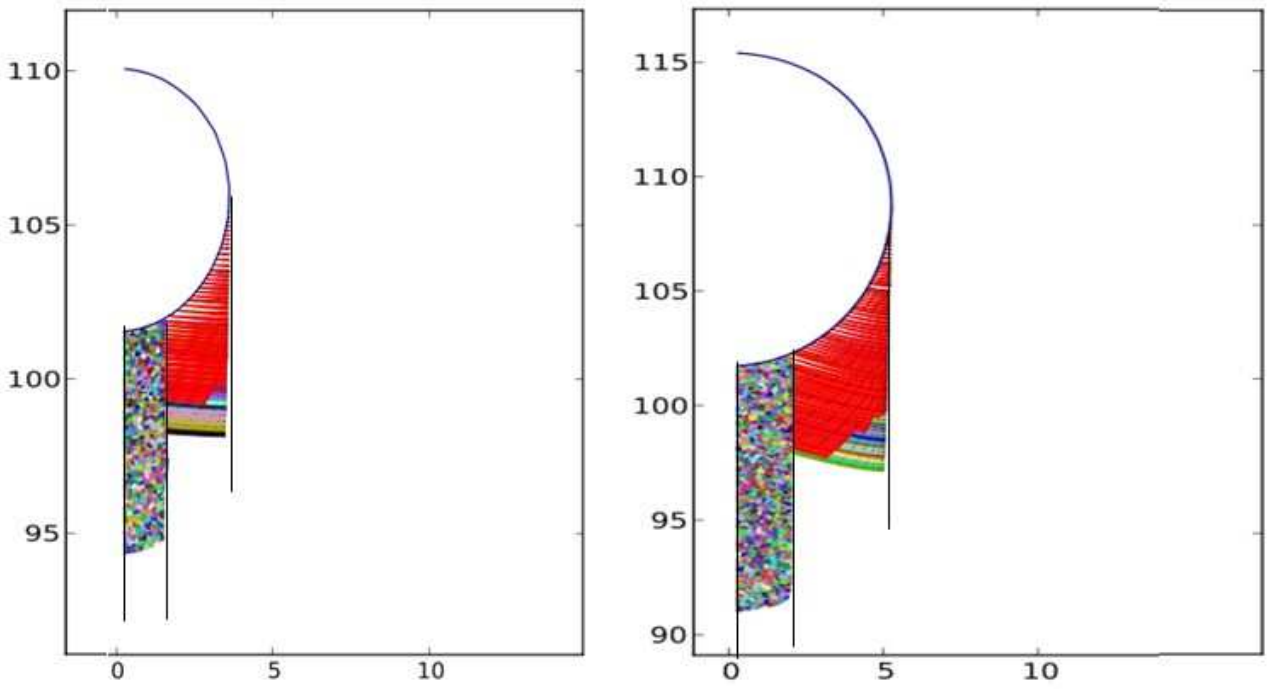

Figure 8: comparison for the two tests left (A) right (B).

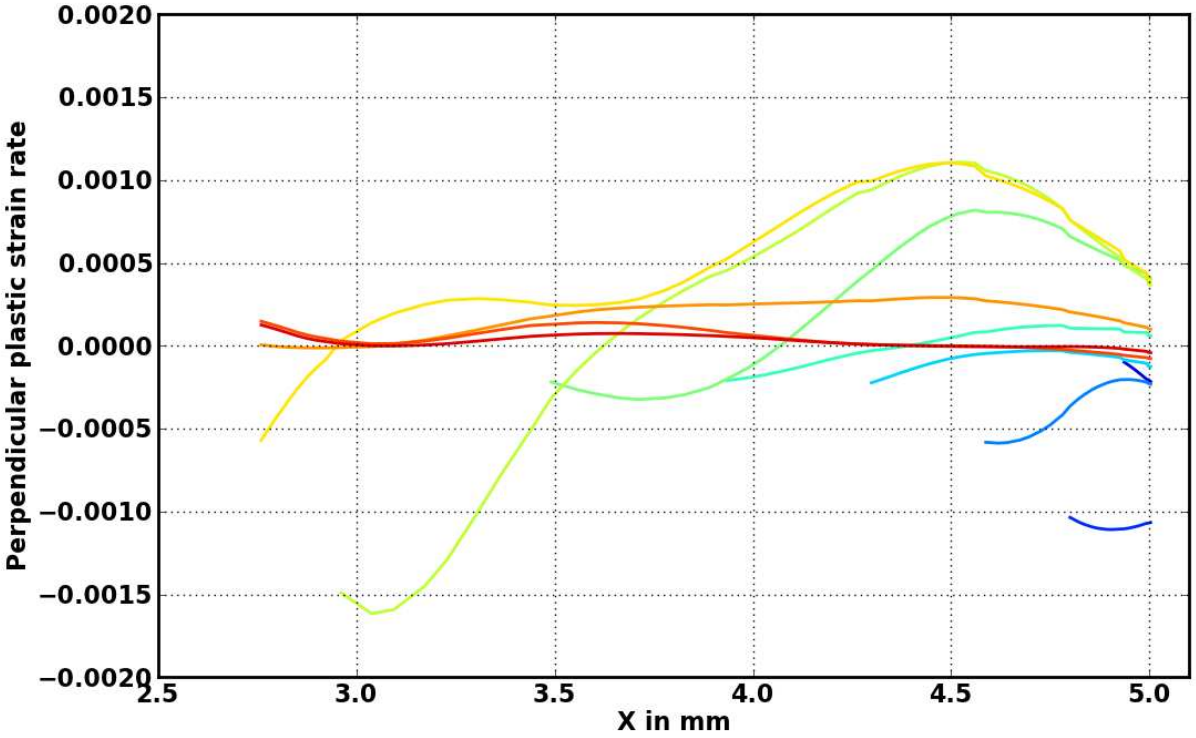

Figure 9: Plastic strain rate perpendicular to the critical grain with time. Blue color are columnar grain initiation whereas red color is for the same columnar grain just before crack onset. Right of the graph correspond to the start of the columnar grain from the base material.

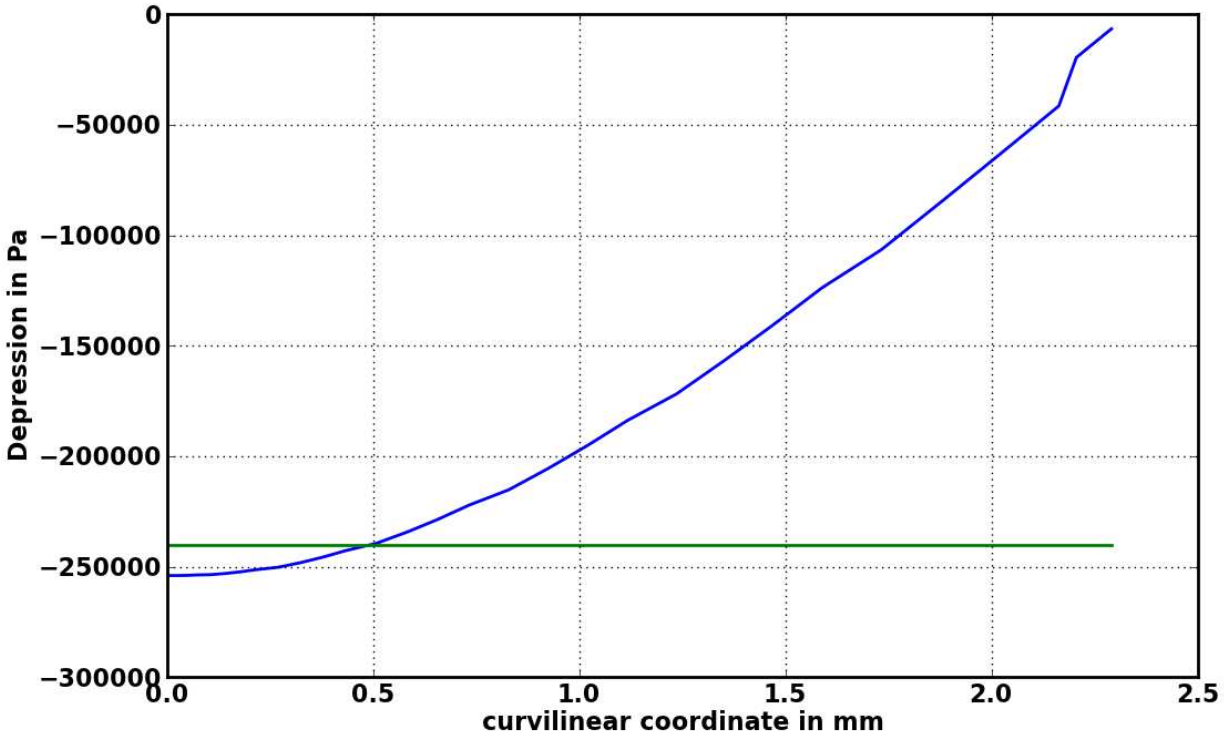

Figure 10 : Depression distribution into a columnar grain. The left is at the foot of the columnar grain ant the right is the part of the grain closer to the weld pool.

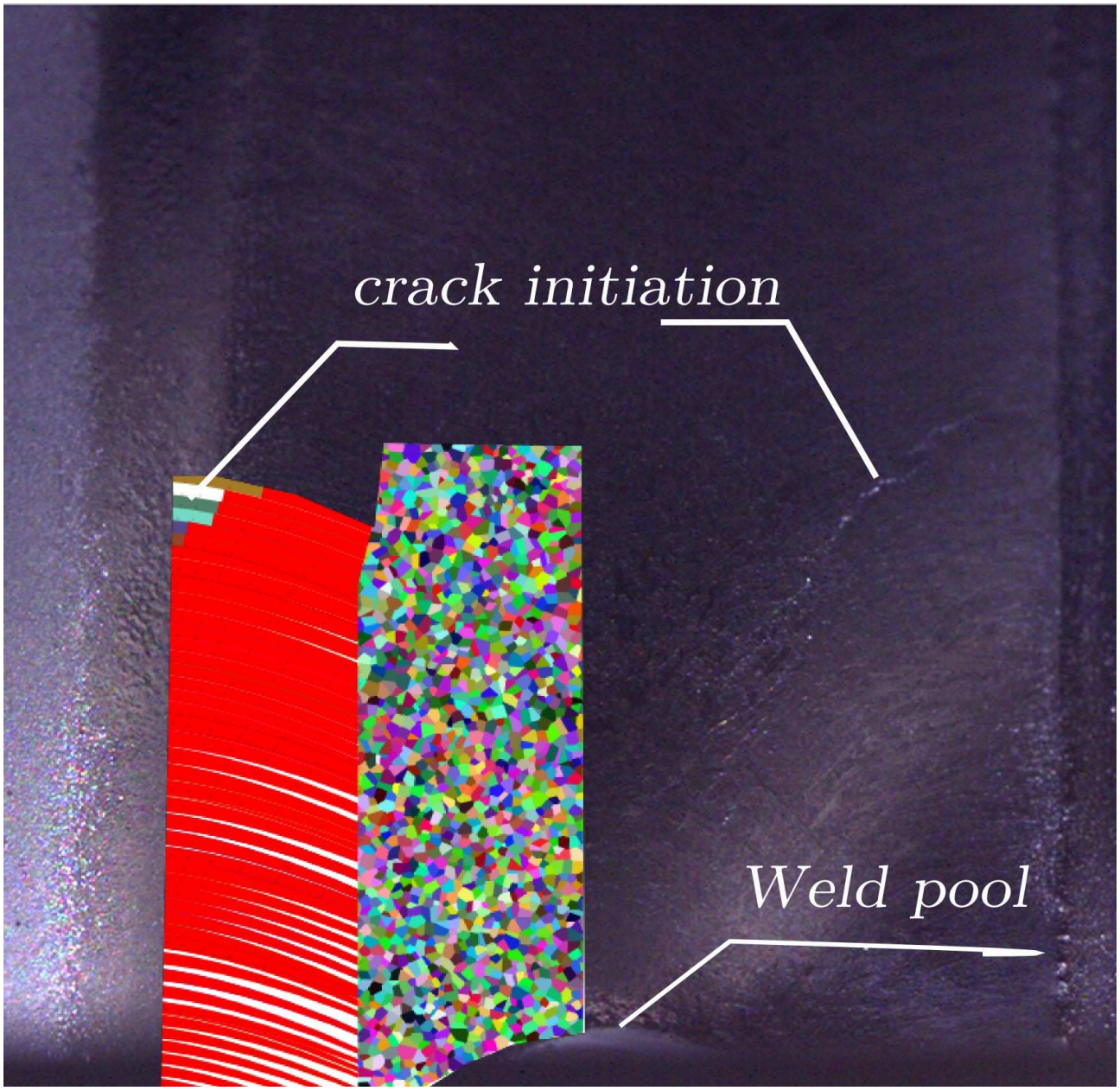

Figure 11: Crack initiation with high speed imaging in 6061 Aluminium alloy compare with crack onset prediction with the simulation and the criteria developed in this paper.

Table 1: process parameters

Test	v(mm/s)	I(A)	U(V)	Imposed displacement (mm)
A	8.3	170	12	0.8
B	8.3	200	12	0.8

Table 2: Geometrical characteristic of the microstructure in the weld pool.

Test	Weld pool width (mm)	Columnar grain length (mm)	Mean angle of columnar grains (°)	Equiaxed grain width (mm)
A	7.2	1.9	6.1	3.4
B	9.2	2.6	14.2	4.1

Table 3: Thermal coefficient

Coefficient	
Density solid(kg.m-3)	2700
Conductivity (W/m.K)	200
Capacity (J/kg/K)	500. (à vérifier)
Density liquid kg/m3	2200

Table 4: Mechanical parameters [10]

Parameter	ambient	500°C
E (Mpa)	70000	68000
V	0.3	0.3
Alpha	27e-6	35e-6
Re(Mpa)	280	80

Table 5: Algorithm for geometrical prediction of the microstructure for each time step

1, Extract temperature field and gradient field from the process simulation:
T_n and ∇T_n

2, Computation of the contour of isotherm melting temperature at . t_n

3, Interpolation of T_n on the melt isotherm of melting temperature

4, Computation of the ratio of equiaxed grains and locate P^n_{CET}

5, Nucleation of columnar and equiaxed grains in the different zones between: t_{n-1} and t_n

6, Growth of columnar grains with eq until the isotherm or the equiaxed zone is reached.

Table 6: Numerical procedure to compute the pressure along the each columnar grain predicted before.

1, construct element based on equation all along the columnar grain
2, extrapolate thermal field and plastic strain rate tensor at gauss points.
3, compute perpendicular plastic strain rate and solid fraction derivative at gauss points
4, compute elementary matrices and right hand side elementary matrix
5, assemble all elementary matrices and right hand side
6, impose atmospheric pressure at tip of the columnar grain
7, solve for pressure at nodes

Table 7 : Weld pool and microstructure prediction

Test	Weld pool width (mm)	Columnar grain length (mm)	Mean angle of columnar grains (°)	Equiaxed grain width (mm)
A	7	1.9	6.	2.2
B	10	2.6	14.	4.8